Ramifications of intermediate-scale ionospheric structure for tomographic reconstruction using two-dimensional simulation. AGU Poster SA21B-2019

Charles L Rino
http://chuckrino.com/wordpress/

December 10, 2013

Abstract

Global observation of the GPS satellite constellation for ionospheric diagnostics is now a worldwide activity driven by both practical and scientific objectives. Diagnostic methods exploit a frequency-dependent phase change, which is proportional to the path-integrated electron density (TEC). However, intermediate-scale structure causes a stochastic modulation of the GPS signals (scintillation), which is a nuisance for data assimilation. Indeed, sufficiently strong propagation disturbances degrade TEC and ultimately disrupt GPS operations altogether. However, the physical processes that generate intermediate-scale structure are intimately part of ionospheric physics. In the best of all possible worlds irregularity identification and classification would be an integral part of ionospheric diagnostics.

This paper explores the relation between intermediate-scale structure and tomographic reconstruction as a means of interpreting propagation measurements. To provide a representative but computationally manageable analysis framework, two-dimensional simulations of highly elongated structure are used. The challenge is to provide representative realizations of large- and intermediate-scale structure.

1 Introduction

The entire earth's ionosphere is accessible to monitoring via GPS signals received by low-earth-orbiting (LEO) satellites and LEO or GPS satellite signals received by fixed ground stations. The GPS-to-LEO observations intercept the ionosphere preceding or following occultations. By measuring the refraction that occurs during the occultations a formal inversion operation extracts an estimate of the electron density height profile. Additionally, multi-station observations can be processed to estimate structure via tomographic reconstruction.

Interpretation of remote sensing observations starts with a *forward* calculation of the interaction of the transmitted electromagnetic (EM) wave with the intervening medium. The theory of EM wave propagation in weakly inhomogeneous (transparent) media is well understood. Hi fidelity forward computations can be performed with structure realizations that contain large-scale deterministic background structures and stochastic intermediate-scale structure with scales from hundreds of kilometers to hundreds of meters.

In the absence of scintillation, which is a manifestation of enhanced intermediate scale structure, signal phase is proportional to the path integral along the ray connecting the source to the receiver. This simple relation makes it possible to obtain a linear relation between measured phase and the in situ contributions along the source-to-receiver path. A collection of discrete measurements can be represented by a linear relation between the measurement vector and a vector arrangement of parameters that define local structure contributions. A model matrix is defined by the ray geometry and the formal representation of the in situ structure. For typically accessible geometries, the model matrix is poorly conditioned. Thus, reconstructions must constrain the solution space, which is comprised of all configurations that support the measurements. Constrained reconstructions are not unique. Moreover, they acutely sensitive to model-matrix errors. Even so, so called tomographric reconstruction is playing an increasingly important role in ionospheric physics.

This paper uses two-dimensional simulations to explore the accessible scale range for ionospheric tomographic reconstruction and is sensitivity to propagation disturbances. It is well known that scintillation, which is a manifestation of enhanced intermediate-scale structure, induces a more complicated relation between measurements and the contributing path-integrated structure. In effect, the very process that makes remote sensing possible distorts the tomographic measurement ideal. To introduce the problem, consider the formal process by which electromagnetic (EM) waves interact with small local inhomogeneities. Let $\psi(x;\varsigma)$ represent the complex field at frequency f. The x direction here is the propagation axis. The variable ς is in the plane perpendicular to the propagation direction. In free space one can show by direct computation that the following propagation operation satisfied the Helmholz equation exactly:[1]

$$\psi(x+x_m;\varsigma) = \iint \widehat{\psi}(x_m;\kappa)\exp\{ikg(\kappa)\,|x-x_m|\} \times \exp\{i\kappa\cdot\varsigma\}\frac{d\kappa}{(2\pi)^2}, \tag{1}$$

where

$$\widehat{\psi}(x_m;\kappa) = \iint \psi(x_m;\varsigma)\exp\{-i\kappa\cdot\rho\}d\rho, \tag{2}$$

[1] Hemholtz equation can be written as

$$\nabla^2\psi + k^2\psi = 0.$$

is the two-dimensional Fourier decomposition of the field at x_m,

$$kg(\kappa) = k\sqrt{1-(\kappa/k)^2}, \tag{3}$$

and $k = 2\pi f/c = 2\pi/\lambda$ is the magnitude of the wavevector

$$\mathbf{k} = [kg(\kappa), \kappa]\,. \tag{4}$$

The limit

$$\lim_{x\to x_m} \left(\psi(x+x_m;\varsigma) - \psi(x_m;\varsigma)\right)/\left(x-x_m\right), \tag{5}$$

defines the differential form of the forward propagation operator:

$$\frac{\partial\psi(x,\varsigma)}{\partial x} = ik\Theta\psi(x,\varsigma). \tag{6}$$

With $\delta n(x,\varsigma)$ representing a local variation in the refractive index, the complete forward propagation equation (FPE) is [1, Chapter 3]

$$\frac{\partial\psi(x,\varsigma)}{\partial x} = ik\Theta\psi(x,\varsigma) + ik\delta n(x,\varsigma)\psi(x,\varsigma). \tag{7}$$

The ideal tomographic relation is realized when the diffraction operator advances the field forward without modification. Formally, the diffraction operator Θ replaced with the identify operator I. The solution to (7) is

$$\psi(L,\varsigma) = \exp\left\{ik\left(L - \int_0^L \delta n(x,\varsigma)dx\right)\right\}. \tag{8}$$

However, a coherent receiver measures phase with respect to a local oscillator. Thus, the field measured by a coherent receiver is

$$\begin{aligned}\psi_k(L,\varsigma) &= \psi(L,\varsigma)\exp\{-ikL\} \\ &= \exp\left\{-ik\int_0^L \delta n(x,\varsigma)dx\right\}.\end{aligned} \tag{9}$$

Rewriting the FPE to generate $\psi_k(L,\varsigma)$ directly,

$$\frac{\partial\psi_k(x,\varsigma)}{\partial x} = ik\left(I-\Theta\right)\psi_k(x,\varsigma) + ik\delta n(x,\varsigma)\psi_k(x,\varsigma). \tag{10}$$

For modeling purposes, ideal tomographic measurements would reproduce solutions to

$$\frac{\partial\psi_k(x,\varsigma)}{\partial x} = ik\delta n(x,\varsigma)\psi_k(x,\varsigma), \tag{11}$$

from which the path-integrated phase can be extracted. There is no measurement that adheres to this ideal exactly. As already noted, the diffraction process that carries the signal to the receiver distorts the signal phase. The amount of distortion depends on the field structure, the operating frequency and the propagation distance. Structure in the intermediate scale range (100 km to 100m) is the source of scintillation above 100 MHz.

1.1 Oblique Incidence

Figure (1) shows a schematic representation of a satellite-to-ground propagation path through a disturbed region. The origin of the reference coordinate system is fixed at some convenient location in the disturbed medium. The ray from the source to the receiving antenna phase centers is a formal reference for computation. The means of centering the computation on the reference path will be described later. However, the FPE is integrated, the geometry and structure configuration is assumed to be frozen. In physical space the time interval is the transmission time from the source to the receiver, which is the primary GPS measurement. It should be noted that the FPE applies to each transmitted frequency separately. The frequency dependence of the refractive index introduces a group delay that must be compensated. With multi-frequency measurements, the ionospheric contribution can be estimated for bias correction and recorded for ionospheric diagnostic measurement, as already noted.

Over short time intervals the satellite motion vector is constant. Over such an interval the time-series measured by a receiver in the observation plane can be interpreted as a translation of the coordinate system through the structure. Drift motion offsets the effective translation velocity. The resulting purely geometric transformations are particularly convenient for interpreting propagation through highly anisotropic field-aligned structure. Most scintillation analyses assume invariant geometry and frozen structure for a period long enough to resolve the frequency content of signal intensity and phase variations. For this type of analysis the satellite motion is effectively replaced by step changes. Allowing the steps to overlap provides common segments to check the magnitude of the changes. Changes within the processing interval distorts the space to time translation and any subsequent interpretation.

1.2 Wavefront Curvature

To fully accommodate propagation from a compact source the field incident upon the structure would be used to initiate the forward integration. However, satellite antenna patterns are difficult to acquire and use because they depend on the attitude of the satellite as well as its location. For a well-designed system, locally spherical incident wave illumination is a good approximation in the absence of distorting multipath reflections. The dominant effect of a spherical incident wavefield is a dilation of the field. The dilation can be accommodated by scaling the transverse measurement grid by the ratio of the product to the sum of the source to reference and reference to ground distances. The limit is a uniform plane-wave field, which is the simplest excitation field. The tomographic computation of the path integration uses the starting and end points of each measurement. In that case, the diverging rays map the spherical wavefronts. For simulations that use uncompensated plane-wave excitation, the rays that defined the path integration are parallel.

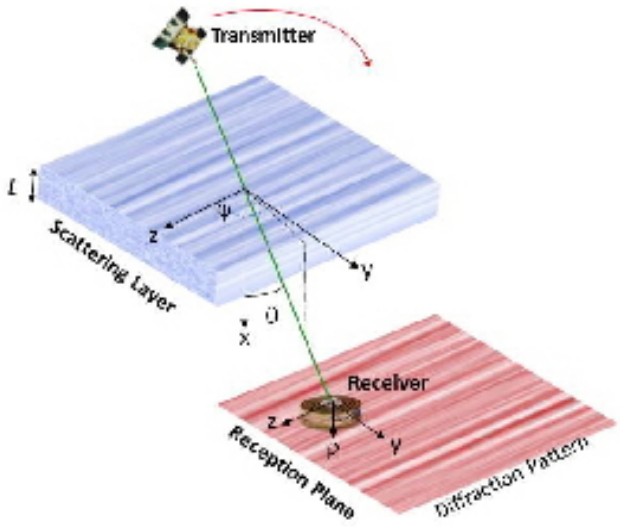

Figure 1: Schematic representation of oblique propagation through highly structure media.

1.3 Structure Models

The final consideration for simulations is the structure model itself. Physics based models can accurately reconstruct the large scale plasma configuration. The distribution of embedded intermediate-scale structure and its power-law characteristics are areas of active research. Moreover, highly field-aligned structure is formally stochastic only in the cross-field direction. Since the focus of this paper is the ramifications of intermediate scale structure on tomographic reconstruction, representative models suffice. Ideally, estimation of local structure would be part of the tomographic inversion process.

2 Propagation Simulations for Tomographic Reconstruction

To solve (10) for the geometry shown in Figure (1) efficiently, the incident field must be confined to a narrow range of propagation angles. Following the example in the Introduction, this is achieved by first centering the incident field on the reference propagation direction:

$$\psi_{\mathbf{k}}(x,\varsigma) = \psi(x,\varsigma)\exp\left\{-ik\left[\cos\theta, \widehat{\mathbf{a}}_{k_T}\right]\right\}, \tag{12}$$

where $\widehat{\mathbf{a}}_{k_T}$ is a unit vector along the transverse projection of the propagation operator. The next step introduces a sliding origin, effectively a continuously displaced coordinate system (CDSC) terminating

$$\mathbf{R}_0(x) = \left[x, \tan\theta\widehat{\mathbf{a}}_{k_T}x\right]. \tag{13}$$

With accommodation for the centering and CCD operations, the diffraction operator becomes

$$\begin{aligned}\psi_{\mathbf{k}}(x,\rho) = \iint \widehat{\psi}_{\mathbf{k}}(0;\kappa)\exp\{i\left(k\cos\theta - g(\kappa+\mathbf{k}_T) + \tan\theta\widehat{\mathbf{a}}_{k_T}\cdot\kappa\right)x\} \\ \times\exp\{i\kappa\cdot\rho\}\frac{d\kappa}{(2\pi)^2}.\end{aligned} \tag{14}$$

In the CDC system (10) becomes

$$\frac{\partial\psi_{\mathbf{k}}(x,\varsigma)(x,\rho)}{\partial x} = ik\left(\cos\theta - \Theta_k\right)\psi_{\mathbf{k}}(x,\varsigma)(x,\rho) + ik\sec\theta\delta n(x,\rho - \tan\theta\widehat{\mathbf{a}}_{k_T}x)\psi_{\mathbf{k}}(x,\varsigma)(x,\rho). \tag{15}$$

The relation between ς and ρ is

$$\rho = \varsigma + \tan\theta\widehat{\mathbf{a}}_{k_T}x. \tag{16}$$

This is a modification of the form given in Chapter 4 of *The Theory of Scintillatio with Applications in Remote Sensing*,[1] which does not include the reference wave offset.

2.1 Refractive Index Realization

The refractive index variation that drives propagation effects is formally represented as

$$n(\rho) = \overline{n}(\rho)(1 + \delta n(\rho)/n_0), \tag{17}$$

where $\overline{n}(\rho)$ represents a deterministic profile function and $(1 + \delta n(\rho)/n_0)$ is a modulation imposed by smaller scale stochastic structure. At frequencies above 100 MHz, the ionospheric refractive index variation is a frequency-dependent mapping of the electron density:

$$n(\rho) \simeq 1 - 2\pi r_e N_e(\rho)/k^2. \tag{18}$$

In phase units,

$$\begin{aligned} k\delta n(\rho) &\simeq -2\pi r_e N_e(\rho)/k \\ &= -\left(r_e c\right) N_e(\rho)/f, \end{aligned} \tag{19}$$

where $r_e = 2.819740289e^{-15}m$ and c is the speed of lignt (299792458 mps). It is conveneint to write the phase perturbation in terms of a conversion factor K defined as

$$\begin{aligned} K &= \frac{r_e c}{2\pi} \times 10^{16} \\ &= 1.3454 \times 10^9. \end{aligned} \tag{20}$$

An change of 10^{16} electrons/m^3 is called a TEC unit. In TEC units

$$k\delta n(\rho) = -2\pi K N_e(\rho)/f \text{ radians/Hz/m} \tag{21}$$

where ω is the frequency in radians per second. It is customary to use this relation to convert measured pathe-integrated phase to TEC units:

$$TEC = -f\overline{\phi}/\left(2\pi K\right) \tag{22}$$

The deterministic component $\overline{n}(\rho)$ can be constructed from physics-based models. The simplest form is a Chapman layer. The structure component is usually constructed by imposing a power law weighting on uncorrelated samples via Fourier transformation. This necessarily produces uniform statistics over the transformation volume. More realistically, the structure would vary over the volume in respons to the background configuration. A configuration space model can accommodate such variation as well as field-aligned anisotropy. For the purposes of this initial study, only uniform stochastic structure will be use.

3 Two Dimensional Propagation

Figure 2 is a schematic representation of a two dimensional configuration. The the solution of the FPE in continuously displaced coordinates captures the structure within the parallelogram that defines the displaced coordinate boundaries

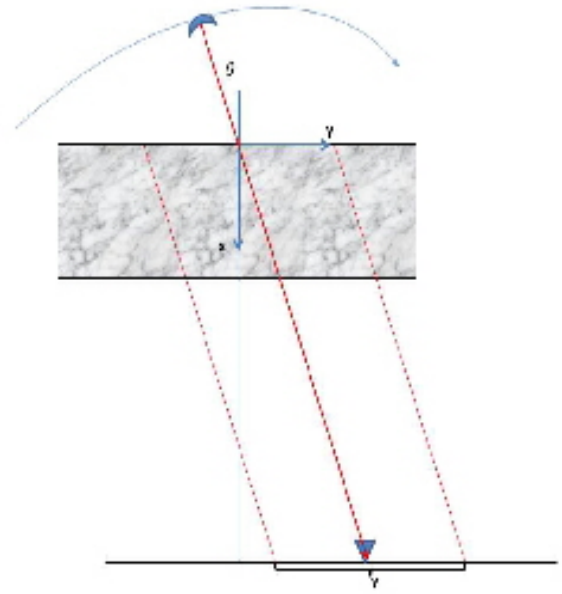

Figure 2: Scematic representation of planar geometry for tomographic reconstruction.

relative to the source direction. Solving the FPE generates a realization of the field over an extended region centered on the reference ray, $-Y/2 <= y - x\tan\theta < Y/2$. The central ray and the two bounding rays are shown in red. As noted in the introduction, for plane-wave excitation, the ray paths are parallel.

The parallel rays that connect each point in the measurement plane at the exit plane of the layer are defined by their termination point y,

$$\phi\left(y,\theta\right) = \frac{2\pi}{\lambda}\sec\theta\int_0^L \delta n(\eta, y-\eta\tan\theta)d\eta. \tag{23}$$

Ideal tomographic reconstruction would be based on the following linear mapping relation

$$\phi_k^j = \frac{2\pi}{\lambda}\sec\theta\int_0^L \delta n(\eta, k\Delta y-\eta\tan\theta_j)d\eta \tag{24}$$

where k is parallel ray index and j is the receiver index.

3.1 Diffraction

To calculate the wave field at the observation plane, the following form of the FPE is used:

$$\frac{\partial \psi_k(x,y)}{\partial x} = ik(I - \Theta_k)\psi_k(x,y) + ik\sec\theta\delta n(x, y - \tan\theta x)\psi_k(x,y). \tag{25}$$

where

$$\Theta\psi_k(x,y) = \int \widehat{\psi}_k\left(x_n;\kappa_y\right)\exp\left\{i\left(\left(kg(\kappa_y + k\sin\theta) - k\cos\theta + \tan\theta\kappa_y\right)\right)dx\right\}$$
$$\times \exp\left\{i\kappa_y y\right\}\frac{d\kappa_y}{2\pi}. \tag{26}$$

For split-step integration, the phase perturbation at the exit plane of each propagation step is computed from the electron density realization converted to refractive index variations $\delta n(x,y)$

$$\phi\left(y,\theta\right) = \frac{2\pi}{\lambda}\sec\theta\int_x^{x+\Delta x}\delta n(\eta, y - \eta\tan\theta)d\eta \tag{27}$$

3.1.1 Edge Discontinuities

At each propagation step the intercepted structure increment must centered on the reference propagation direction per (27). The shift could be accommodated by increasing the size of the realization, but truncating the new data in the computation window introduces edge discontinuities. Edge discontinuities initiate spurious propagation into the propagation space. Tapering the illumination field suppresses the edge contributions, although the taper is artificial. Ideally, a non-reflecting boundary condition would be imposed, but the procedures are complicated.[2] A simpler procedure uses a period shift of the structure, which is automatic if the shift is implemented by imposing a phase ramp on the DFT. Although periodic structures eliminate edge discontinuities, they create their own peculiarities. Over typical layer dimensions the displacement can be large enough to move a central feature to the edge of the data window. The extent of the refractive index realization determines the maximum propagation angle that can be processes without such wraparound, aothough computation for a genuinely periodic structure would be exact.

4 Tomographic Reconstruction

Reconstruction of the in-situ structure from (24) requires a discrete model for $\delta n(\eta, y - \eta\tan\theta)$. A two-dimensional Fourier decomposition provides insight.

[2] Absorbing non-local boundary conditions are discussed in Chapter 8 of Levy [2]

Let

$$\delta n(x,y) = \frac{1}{NM} \sum_{n=-N/2}^{N/2-1} \sum_{m=-M/2}^{M/2-1} \widehat{\delta n}_{nm} \exp\left\{i\left(n\Delta\kappa_x x + m\Delta\kappa_y y\right)\right\}, \tag{28}$$

where $\Delta\kappa_x = 2\pi/\left(N\Delta x\right)$ and $\Delta\kappa_y = 2\pi/\left(M\Delta y\right)$. Upon substituting (28) into (24) it follows that

$$\begin{aligned}
\phi_k^j &= \frac{2\pi}{\lambda}\sec\theta\Delta x \sum_{n'=0}^{N-1} \delta n(n'\Delta x, k\Delta y - n'\Delta x\tan\theta_j) \\
&= \frac{2\pi}{\lambda}\sec\theta\Delta x \frac{1}{NM} \sum_{n=-N/2}^{N/2-1} \sum_{m=-M/2}^{M/2-1} \widehat{\delta n}_{nm} \\
&\times \sum_{n'=0}^{N-1} \exp\left\{2\pi i n'/N\left(n - m\left(\Delta\kappa_y/\Delta\kappa_x\right)\tan\theta_j\right)\right\} \exp\left\{2\pi i m/M\left(k\Delta y\right)\right\}.
\end{aligned} \tag{29}$$

Evaluating the summation over n' and computing the Fourier decomposition of $\phi\left(y,\theta\right)$ over the y variable leads to a linear relation for each horizontal mode index by m:

$$\widehat{\phi}\left(m\Delta\kappa_y,\theta\right) = \left[\frac{1}{N}\sum_{n=-N/2}^{N/2-1} \Phi\left(n, m\left(\Delta\kappa_y/\Delta\kappa_x\right)\tan\theta\right)\widehat{\delta n}_{nm}\right] \tag{30}$$

where

$$\Phi_N\left(n, m\gamma\right) = \frac{2\pi\sec\theta L}{\lambda} \frac{\exp\left\{2\pi i\left(n - m\gamma\right)\right\} - 1}{N\exp\left\{2\pi i\left(n - m\gamma\right)/N\right\} - 1}. \tag{31}$$

The (30) summation in square brackets can be written as the vector inner product:

$$\widehat{\phi}_m^j = \frac{1}{N}\mathbf{\Phi}_m^{jT}\widehat{\delta\mathbf{n}}_m, \tag{32}$$

where $\widehat{\phi}_m$ is an $N_j \times 1$ indexed column vector, and Φ_m is an $N_j \times N$ indexed matrix with elements $\Phi_N\left(n, m\left(\Delta\kappa_y/\Delta\kappa_x\right)\tan\theta_j\right)$. The linear relation applies independently to each indexed y Fourier coefficient. The m-indexed systems of linear equations comprise a model for tomographic reconstruction.

4.1 SVD Reconstruction

The Fourier coefficients can be estimated from the data vectors $\widehat{\phi}_m$. However, the model matrix is generally poorly conditioned. Single-valued decomposition (SVD) provides a means of extracting an approximate solution that most closely represents the model relation. Applying SDV, Φ_m can be written as

$$\Phi_m = USV', \tag{33}$$

where S is diagonal with the same dimension as Φ_m, U is a unitary matrix with the column dimension, and V is a unitary matrix with the row dimension. A modified pseudo inverse is constructed replacing the diagonal elements with

$$S'_n = S(n)/\left(S^2(n) - \epsilon^2\right), \tag{34}$$

whereby

$$\Phi_m^{-1} = VS'U'. \tag{35}$$

References

[1] Charles L. Rino. *The Theory of Scintillation with Applications in Remote Sensing*. John Wiley and Sons, Inc., New York, 2011.

[2] Mireille Levy. *Parabolic Equation Methods for Electromagnetic Wave Propagation*. Institute of Electrical Engineers, United Kingdom, 2000.